

MULTI DOMAIN CT METAL ARTIFACTS REDUCTION USING PARTIAL CONVOLUTION BASED INPAINTING

Artem Pimkin^{1,2}, Alexander Samoylenko², Natalia Antipina³
Anna Ovechkina⁴, Andrey Golanov³, Alexandra Dalechina⁵ and Mikhail Belyaev¹

¹ Skolkovo Institute of Science and Technology, Moscow, Russia

² Moscow Institute of Physics and Technology, Moscow, Russia

³ N. N. Burdenko National Medical Research Center of Neurosurgery

⁴ Lomonosov Moscow State University

⁵ The Gamma Knife Center at the N. N. Burdenko Institute of Neurosurgery
artem.pimkin@phystech.edu, samojlenko.ai@phystech.edu,
m.belyaev@skoltech.ru

ABSTRACT

Recent CT Metal Artifacts Reduction (MAR) methods are often based on image-to-image convolutional neural networks for adjustment of corrupted sinograms or images themselves. In this paper we are exploring the capabilities of a multi domain method which consists of both sinogram correction (projection domain step) and restored image correction (image domain step). Moreover, we propose a formulation of the first step problem as a sinogram inpainting which allows us to use methods of this specific field such as partial convolutions. The proposed method allows to achieve state-of-the-art (-75% MSE) improvement in comparison with a classic benchmark - Li-MAR.

Index Terms— Convolutional Networks, Computed Tomography (CT) images, Metal Artifacts Reduction, Sinogram Inpainting, Partial Convolutions

1. INTRODUCTION

Computed Tomography is a commonly used imaging method in disease diagnosis and radiation therapy for dose distribution calculation based on the electron density of the irradiated tissues and patient-specific anatomy. High-density objects (e.g., containing metal) may occur in the area of interest and strongly affect the attenuation of X-Rays that may lead to distortion of the final image reconstructed from an inconsistent sinogram [1]. These image artifacts could have a significant impact on the dose distribution accuracy and reduce the visibility of organs and structures close to the metal objects [2], [3].

given an input 3D tensor that represents a CT scan corrupted by the presence of high density objects, generate a corresponding CT image with suppressed artifacts. different methods have been in development during the last 40 years

[4]. The majority of the proposed solutions can be divided into two large groups based on the domain of the input data:

1. Algorithms consisting of removal of the high density area from sinogram with further reconstruction based on the other parts of image, also known as projection-based, e.g. Li-MAR [5]. Nowadays this problem may be solved using image to image deep learning based approaches (e.g. [6]).
2. Image-based solutions that use image-to-image networks and reduce artifacts directly on the scans (e.g. [7]).

In this paper we propose a deep learning based method that combines both approaches described above: it consists of two models that process the image representation in two domains. The first inpainting model is responsible for removal of the distorted metal trace from the sinogram. The second refining model corrects the residual artifacts after restoration of the image. In this work we have successfully verified the following statements:

1. Refining model improves the quality of the result since even minor inconsistencies in the sinogram may lead to significant artifacts on the restored image.
2. Sinogram adjustment via inpainting model may simplify the problem for direct image-to-image refining model.

Besides, we formulate the problem of restoration of the corrupted area of sinogram directly as image inpainting which in turn allows to use state-of-the art approaches for this step, e.g. partial convolution based neural network (which was introduced in [8] for inpainting of irregular holes).

For a training of deep learning models we propose a high density random objects generation pipeline that allows us to

solve a problem of natural paired data absence. Also it allows us to avoid a problem of domain adaptation since shapes of generated objects are structurally close to the real shapes (more details in Section 2.2).

Li-MAR is a classic MAR method which consists of linear interpolation for missing data within the metal trace. For this reason, we chose it as our reference. Also it allows us to compare quality of our approach with other works using relative difference between model and Li-MAR performances as a metric. We compared the performance in these terms with FCN-MAR[9], Deep-MAR[10] and CNN-MAR[11] as one of the most popular and recent deep learning based methods of metal artifact reduction.

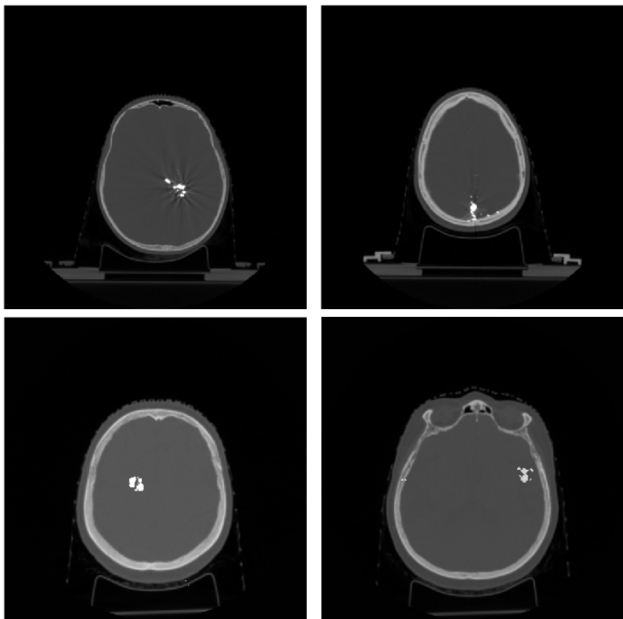


Fig. 1. Example of real shapes of high density objects (above) and shapes generated via proposed pipeline (below).

2. PROPOSED SOLUTION

The main idea of the proposed solution is to combine both image-based and projection-based approaches. The first step is the removal of the metal trace from sinogram with restoration of deleted area (projection domain step). The second step is the elimination of residual artifacts from the restored image (image domain step). More accurate formulation of the pipeline is further in Section 2.1.

2.1. Structure

Firstly, it is important to mention that we implemented slice by slice pipeline due to avoidance of data spatial inconsistencies e.g. different spacing between slices. Thus, we propose the following algorithm structure for each of corrupted slices:

1. Cut a mask of the high density object using threshold (since CT voxel intensities represents its density). This is a common method of detection of such objects (e.g [10]).
2. Obtain sinograms for the corrupted image and for the mask of the object using Radon transform.
3. Crop the sinogram according to the transformed mask.
4. Restore cropped sinogram area using inpainting model. Ideally it has to match the sinogram of the image with the absence of both high density object and artifacts caused by it.
5. Restore image from obtained sinogram.
6. Adjust the image to remove residual artifacts using refining model.
7. Restore the high density object using the mask from step 1.

At steps 4 and 6 we are using convolutional neural networks as described in Section 2.3. To measure the effectiveness of the proposed algorithm in comparison with only sinogram inpainting and direct image to image model we have also trained the same pipeline without step 4 and step 6 respectively. More details on the pipeline and training loops are shown in Figure 2.

2.2. Synthetic data

Due to absence of the natural paired data we have used CT scans of the patients with no such high density objects on the scan and hence without artifacts caused by them for creation of the synthetic dataset. To create synthetic dataset we have built a random object generator such that generated objects had a similar structure as a real high density objects on head CT scans. To achieve this we used the following algorithm:

1. Select a uniformly random size (up to 10% of the linear size of the image) of a volume where object will be placed.
2. Put a uniformly random (from 1 to 25) number of geometrical structures (ball, octahedron, parallelepiped) of linear size up to 10 pixels into this volume.
3. Merge them using morphological closing operation to obtain a random shaped objects or a small set of them.
4. Put into the volume up to 30 geometrical structures of small size (from 1 to 3 pixels) to obtain an object with outliers.
5. Select a position of the obtained object randomly (via uniform 2D distribution) so that the overlap between the mask and the brain is $\geq 95\%$.
6. Repeat the process up to 10 times to obtain a scan with multiple objects

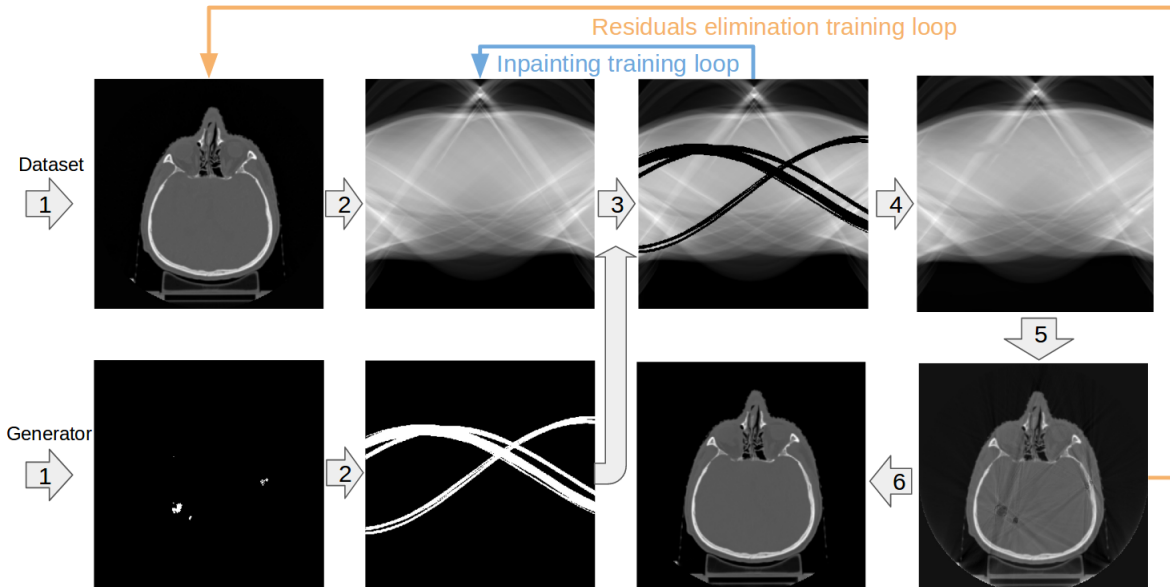


Fig. 2. Training pipeline. Step 1 on the figure represents training version of the first step of the algorithm replaced by generated object and uncorrupted scan instead of segmentation.

Figure 1 shows examples of real and generated objects. Using that algorithm for each of 24 patients (more details in Section 3) we created 30 differently distributed object masks with an approximate depth of 90 slices per sample on average.

2.3. Architectures

For deep learning problems formulated above we used the following architectures:

UNet[12] - model with that architecture won ISBI Challenge: Segmentation of neuronal structures in EM stacks. It was effective even on small amount of data and also performed well in task of metal artifacts reduction on sinograms (e.g. [6]) as well as in direct image to image artifacts removal process (e.g. [7]). In our case we use a model with this architecture for the step 6 of our algorithm - reduction of the residual artifacts on the images.

UNet with partial convolutions - this architecture differs from the UNet mentioned above with convolutions that were replaced by partial convolutions [8] which are masked and renormalized to be conditioned only on the pixels that are not masked. In this work since we formulate the problem of sinogram correction directly as inpainting it allowed us to use this method for that part of pipeline as the state-of-the-art in the field.

3. EXPERIMENTAL SETUP

Data. The initial dataset consists of 24 CT brain scans taken for radiation therapy planning. Each scan is represented by a 3D tensor of shape $512 \times 512 \times N$, where N is the number

of axial slices varying from 130 to 210. Also a set of 47 corrupted scans with the same characteristics was used for visual validation of the solution. The data was divided into three parts patientwisely: training set for the first model, training set for the second model, testing set.

Preprocessing. All input images for both sinogram inpainting and restored CT slice residuals reduction were linearly normalized to fit into $[0, 1]$ window. Such a simple preprocessing was used to maintain the physical sense of voxel intensities.

Metrics. We used a standard MAE (Mean Absolute Error), MSE (Mean Squared Error) and SSIM (Structural Similarity) metrics to measure quality of the final result on the CT scans.

Training. For our full pipeline and approaches comparison we end up with training 3 models: sinogram inpainting (UNet with partial convolutions), residual artifacts elimination (UNet) and image-to-image model for pipeline without inpainting step (Unet). All of the models mentioned above were trained using Adam optimizer with initial learning rate of $5 \cdot 10^{-3}$.

For sinogram inpainting UNet with partial convolutions was trained for 500 epochs with multiplication of the learning rate by 0.5 on each of the following epochs: 100, 200, 300 and multiplication by 0.1 on 400, 450, 475 and 490 epochs respectively.

Models with plain UNet architecture both were trained for 200 epochs with 0.5 learning rate multiplication on 100, 150 and 175 epochs.

All models were created and trained using PyTorch frame-

work and DPipe¹ for configurations management and experiments setup.

4. RESULTS AND CONCLUSION

Test metrics of inpainting-only, image-to-image only, Li-MAR as a classic benchmark and the proposed method are represented in Table 1.

Algorithm	MAE (Hounsfield units)	MSE (HU ²)	SSIM
Li-MAR	26.6	3282	0.94
Inpainting-only	22.0	10170	0.94
Image-to-image only	14.5	2064	0.97
Proposed algorithm	9.6	831	0.99

Table 1. Comparison between one step methods, Li-MAR and two step method in terms of MAE and SSIM between the final output and test set

Here we can see a significant (56%) decrease of MAE between inpainting-only method and the proposed solution. Thus we can conclude that image-to-image network can successfully remove residual artifacts and increase quality of result model. We obtain a huge MSE and relatively small MAE for inpainting model due to inhomogeneity of its errors caused by sinogram inconsistency. On the other hand, we can see a decrease of MAE of 34% between image-to-image only method and our two-step approach. This confirms our hypothesis that sinogram inpainting as preprocessing greatly simplifies the task for the image-to-image model. Moreover the proposed solution significantly outperforms Li-MAR by 64% in terms of MAE.

Table 2 shows a relative drop of MSE reported in different papers in comparison with reported Li-MAR score and provides us an understanding of relatively good performance of the proposed model.

Algorithm	MSE drop
Li-MAR [5]	0.0%
FCN-MAR [9]	-52.2%
Deep-MAR [10]	-58.5%
CNN-MAR [11]	-71.1%
Proposed algorithm	-75.5%

Table 2. Relative drop compared to Li-MAR performance.

Figure 3 shows examples of our algorithm and Li-MAR work on a real CT scans of the patients with high density objects that cause artifacts on the images. It is visible in the brain window that model restores distinguishable brain structures well.

In this paper we present a state-of-the-art multi domain deep learning procedure that consists of sinogram completion and additional adjustment after inverse Radon transform. The

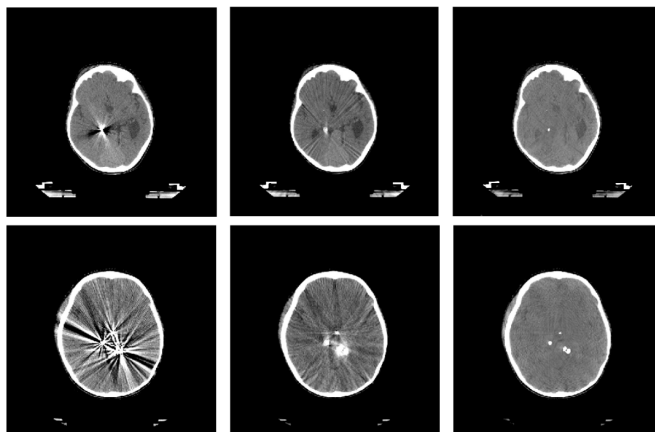


Fig. 3. Examples of processing real corrupted CT scan with intensities in brain window (40+-80 HU). From left to right: original image, Li-MAR output, output of proposed solution. Each row corresponds to the different patient.

results of our experiments show the effectiveness of the proposed approach compared to one step algorithms. Thus qualitative and quantitative analysis show an application potential of the proposed method and the next step of our research is going to be a clinical validation on the dose calculations for radiosurgery planning.

The results have been obtained under the support of the Russian Foundation for Basic Research grant 18-29-26030.

5. REFERENCES

- [1] F. Boas and D. Fleischmann, “Ct artifacts: causes and reduction techniques,” *Imaging in Medicine*, vol. 4, no. 2, pp. 229–240, 2012.
- [2] D. Giantsoudi, B. De Man, J. Verburg, A. Trofimov, Y. Jin, G. Wang, L. Gjestebj, and H. Paganetti, “Metal artifacts in computed tomography for radiation therapy planning: dosimetric effects and impact of metal artifact reduction,” *Physics in Medicine & Biology*, vol. 62, no. 8, pp. R49, 2017.
- [3] D. G Kovacs, L. A Rechner, A. L Appelt, A. K Berthelsen, J. C Costa, J. Friborg, G. F Persson, J. P. Bangsgaard, L. Specht, and M. C Aznar, “Metal artefact reduction for accurate tumour delineation in radiotherapy,” *Radiotherapy and Oncology*, vol. 126, no. 3, pp. 479–486, 2018.
- [4] L. Gjestebj, B. De Man, Y. Jin, H. Paganetti, J. Verburg, D. Giantsoudi, and G. Wang, “Metal artifact reduction in ct: where are we after four decades?,” *IEEE Access*, vol. 4, pp. 5826–5849, 2016.

¹https://github.com/neuro-ml/deep_pipe

- [5] W. A Kalender, R. Hebel, and J. Ebersberger, "Reduction of ct artifacts caused by metallic implants.," *Radiology*, vol. 164, no. 2, pp. 576–577, 1987.
- [6] H. S. Park, Y. E. Chung, S. M. Lee, H. P. Kim, and J. K. Seo, "Sinogram-consistency learning in ct for metal artifact reduction," *arXiv preprint arXiv:1708.00607*, 2017.
- [7] H. Suk Park, S. Min Lee, H. Pyung Kim, and J. Keun Seo, "Machine-learning-based nonlinear decomposition of ct images for metal artifact reduction," *arXiv preprint arXiv:1708.00244*, 2017.
- [8] G. Liu, F. A Reda, K. J Shih, T.-Chun Wang, A. Tao, and B. Catanzaro, "Image inpainting for irregular holes using partial convolutions," in *ECCV*, 2018.
- [9] M. Usman Ghani and W. Karl, "Deep learning based sinogram correction for metal artifact reduction," *Electronic Imaging*, vol. 2018, no. 15, pp. 472–1, 2018.
- [10] M. Usman Ghani and W. Clem Karl, "Fast enhanced ct metal artifact reduction using data domain deep learning," *IEEE Transactions on Computational Imaging*, 2019.
- [11] Y. Zhang and H. Yu, "Convolutional neural network based metal artifact reduction in x-ray computed tomography," *IEEE Transactions on Medical Imaging*, vol. 37, no. 6, pp. 1370–1381, 2018.
- [12] O. Ronneberger, P. Fischer, and T. Brox, "U-net: Convolutional networks for biomedical image segmentation," in *International Conference on Medical image computing and computer-assisted intervention*, 2015, pp. 234–241.